

Automated Deterministic Auction Design with Objective Decomposition

Zhijian Duan^{1,*}, Haoran Sun^{1,*}, Yichong Xia^{1,#}, Siqiang Wang^{1,#},
 Zhilin Zhang², Chuan Yu², Jian Xu², Bo Zheng², Xiaotie Deng¹

¹Peking University ²Alibaba Group

zjduan@pku.edu.cn, {sunhaoran0301, xiayc, smswangsiqiang}@stu.pku.edu.cn,
 {zhangzhilin.pt, yuchuan.yc, xiyu.xj, bozheng}@alibaba-inc.com,
 xiaotie@pku.edu.cn

Abstract

Identifying high-revenue mechanisms that are both dominant strategy incentive compatible (DSIC) and individually rational (IR) is a fundamental challenge in auction design. While theoretical approaches have encountered bottlenecks in multi-item auctions, there has been much empirical progress in automated designing such mechanisms using machine learning. However, existing research primarily focuses on randomized auctions, with less attention given to the more practical deterministic auctions. Therefore, this paper investigates the automated design of deterministic auctions and introduces OD-VVCA, an objective decomposition approach for automated designing Virtual Valuations Combinatorial Auctions (VVCAs). Firstly, we restrict our mechanism to deterministic VVCAs, which are inherently DSIC and IR. Afterward, we utilize a parallelizable dynamic programming algorithm to compute the allocation and revenue outcomes of a VVCA efficiently. We then decompose the revenue objective function into continuous and piecewise constant discontinuous components, optimizing each using distinct methods. Extensive experiments show that OD-VVCA achieves high revenue in multi-item auctions, especially in large-scale settings where it outperforms both randomized and deterministic baselines, indicating its efficacy and scalability.

1 Introduction

Finding high-revenue mechanisms that are both *dominant strategy incentive compatible* (DSIC) and *individually rational* (IR) is a fundamental problem in auction design, where DSIC and IR mechanisms incentivize bidders to truthfully report their valuations and ensure they receive non-negative utilities by doing so. While Myerson [1981] characterized the optimal design for single-item auctions, theoretical approaches have faced significant challenges in general multi-item cases [Dütting et al., 2023]. Consequently, there has been much progress in automated auction design, which formulates a constrained optimization problem and empirically seeks high-revenue mechanisms using machine learning [Sandholm and Likhodedov, 2015, Dütting et al., 2019].

Existing research on the automated design of general multi-item auctions primarily focuses on randomized auctions, which produce randomized allocation outcomes [Dütting et al., 2019, Curry et al., 2020, Peri et al., 2021, Rahme et al., 2021b,a, Duan et al., 2022, Ivanov et al., 2022, Curry et al., 2023, Duan et al., 2023], with deterministic auctions receiving less attention. However, deterministic auctions offer practical advantages over randomized ones in real-world applications, because deterministic allocations are more interpretable and easier to implement, leading to widespread adoption in online advertising [Edelman et al., 2007, Liu et al., 2021, Li et al., 2024]. Motivated by these practical considerations, this paper investigates the automated design of deterministic mechanisms for general multi-item auctions.

The automated design of deterministic mechanisms for general multi-item auctions faces two main challenges. Firstly, *scalability* is a significant concern. This is because presently, the most effective

*Equal contribution.

#Equal contribution.

approach to ensuring DSIC and IR in automated deterministic auction design is to constrain the mechanism to Affine Maximizer Auctions (AMAs) [Roberts, 1979]. AMAs generalize Vickrey-Clarke-Groves (VCG) auctions [Vickrey, 1961] by assigning weights to each bidder and boosting each candidate allocation to achieve higher revenue than VCG while maintaining DSIC and IR. However, AMAs boost each candidate allocation, resulting in $O((n+1)^m)$ boost parameters for n bidders and m items, which is exponentially large. Even worse, computing the allocation result of an AMA, which requires finding the winning allocation that maximizes the affine welfare, is NP-Hard [Rothkopf et al., 1998]. Secondly, the revenue function of AMAs is *non-differentiable* with respect to the AMA parameters. This issue, which we will discuss in detail in Section 4.3, arises because the computation of revenue involves searching for the winning allocation among all $(n+1)^m$ deterministic allocations.

To address the scalability and non-differentiability issues of AMA-based automated deterministic auction design, we introduce OD-VVCA, an objective decomposition approach for designing Virtual Valuations Combinatorial Auctions (VVCAs) [Likhodedov et al., 2005, Sandholm and Likhodedov, 2015]. Firstly, we constrain the mechanism to be deterministic VVCAs, a subset of deterministic AMAs that boost each bidder-bundle pair, reducing the parameter space from $O((n+1)^m)$ to $O(n \times 2^m)$. Secondly, since determining the winning allocations of VVCAs remains NP-Hard [Likhodedov et al., 2005], we develop a parallelizable dynamic programming algorithm to solve the problem relatively efficiently. Thirdly, we decompose the objective function, i.e., the revenue of the VVCA, into continuous and discontinuous components. The continuous component is differentiable almost everywhere, allowing us to take its derivative directly. The discontinuous component is a piecewise constant function, and we use Monte Carlo estimation to approximate the gradient of its Gaussian smoothing. Finally, by integrating the gradients from both components, we optimize the VVCA parameters using gradient ascent.

Extensive experiments show that OD-VVCA can achieve higher revenue than deterministic baselines and even randomized AMA-based approaches, particularly in large-scale asymmetric auctions. Additionally, we conduct an ablation study and case studies to showcase the significant benefits that the objective decomposition brings to ZFO-VVCA in terms of revenue and optimization. All these experimental results indicate the effectiveness of our approach.

2 Related Work

Research in automated auction design can be broadly categorized into two threads. The first thread, initiated by RegretNet [Dütting et al., 2019], utilizes ex-post regret as a metric to quantify the extent of DSIC violation. Building upon this concept, subsequent works such as Curry et al. [2020], Peri et al. [2021], Rahme et al. [2021b,a], Curry et al. [2022], Duan et al. [2022], Ivanov et al. [2022] represent auction mechanisms through neural networks. These models aim to achieve near-optimal and approximate DSIC solutions through adversarial training. The advantages of these regret-based methods lie in their ability to attain high revenue, considering a broad class of auction mechanisms. Furthermore, this methodology is generalizable and applicable to various other mechanism design problems, including multi-facility location [Golowich et al., 2018], two-sided matching [Ravindranath et al., 2021], and data markets [Ravindranath et al., 2023]. However, the regret-based methods are not guaranteed to be DSIC, and computing the regret term can be time-consuming. Moreover, all the regret-based methods are designed for randomized auctions.

The second thread is based on Affine Maximizer Auctions (AMAs) [Roberts, 1979], a weighted variation of the Vickrey-Clarke-Groves (VCG) mechanism. AMAs assign weights to each bidder and boost each candidate allocation, enabling them to achieve higher revenue than VCG while maintaining DSIC. This method is particularly well-suited for scenarios with limited candidate allocations [Li et al., 2024]. Furthermore, the sample complexity of AMA has been characterized by Balcan et al. [2016, 2018, 2023]. However, conventional AMAs encounter scalability challenges in multi-item auctions with n bidders and m items, given the total of $(n+1)^m$ deterministic candidate allocations. Additionally, an AMA’s revenue is non-differentiable regarding its parameters, as the computation involves searching for the affine welfare-maximizing allocation. One approach to address these challenges is to restrict the size of candidate allocations to $s \ll (n+1)^m$ and make the candidate allocations learnable [Curry et al., 2023, Duan et al., 2023], leading to randomized candidate allocations. However, the effective size of candidate allocations still grows with an increasing number of bidders and items. As we will discuss in Section 5, this growth results in suboptimal performance in large-scale auctions.

An additional strategy to address the scalability issue of AMA involves further constraining the mechanism to specific subsets, such as Virtual Valuations Combinatorial Auctions (VVCAs) [Likhodedov and Sandholm, 2004, Likhodedov et al., 2005, Sandholm and Likhodedov, 2015], λ -auctions [Jehiel et al., 2007], mixed bundling auctions [Tang and Sandholm, 2012], and bundling boosted auctions [Balcan et al., 2021]. Among these options, VVCAs constitute the most significant subset. Given this, we focus on restricting the mechanism to be VVCAs. However, VVCAs still suffer from the non-differentiability of revenue. Existing VVCA-based algorithms [Likhodedov et al., 2005, Sandholm and Likhodedov, 2015] compute the “gradient” of revenue based on fixed winning allocations, neglecting the influence of VVCA parameters on the winning allocations.

3 Preliminary

Sealed-Bid Auction A sealed-bid auction involves n bidders denoted as $[n] = \{1, 2, \dots, n\}$ and m items denoted as $[m] = \{1, 2, \dots, m\}$. Each bidder i assigns a valuation $v_i(\mathcal{S})$ to every bundle of items $\mathcal{S} \subseteq [m]$ and submits bids for each bundle as $\mathbf{b}_i \in \mathbb{R}^{2^m}$. We assume $v_i(\emptyset) = 0$ for all bidders. In the additive setting, $v_i(\mathcal{S}) = \sum_{j \in \mathcal{S}} v_i(\{j\}) = \sum_{j \in \mathcal{S}} v_{ij}$. The valuation profile $V = (\mathbf{v}_1, \mathbf{v}_2, \dots, \mathbf{v}_n)$ is generated from a distribution D . The auctioneer lacks knowledge of the true valuation profile V but can observe the bidding profile $B = (\mathbf{b}_1, \mathbf{b}_2, \dots, \mathbf{b}_n)$.

Auction Mechanism An auction mechanism (g, p) consists of an allocation rule g and a payment rule p . Given the bids B , $g_i(B)$ computes the allocation result for bidder i , which can be a bundle of items or a probability distribution over all the bundles. The payment $p_i(B) \geq 0$ computes the price that bidder i needs to pay. Each bidder aims to maximize her utility, defined as $u_i(\mathbf{v}_i, B) := v_i(g_i(B)) - p_i(B)$. Bidders may misreport their valuations to gain an advantage. Such strategic behavior among bidders could make the auction result hard to predict. Therefore, we require the auction mechanism to be *dominant strategy incentive compatible (DSIC)*, meaning that for each bidder $i \in [n]$, reporting her true valuation is her optimal strategy regardless of how others report. Formally, a DSIC mechanism satisfies that, for any bidder $i \in [n]$ and any bids of others $B_{-i} = (\mathbf{b}_1, \dots, \mathbf{b}_{i-1}, \mathbf{b}_{i+1}, \dots, \mathbf{b}_n)$, we have $u_i(\mathbf{v}_i, (\mathbf{v}_i, B_{-i})) \geq u_i(\mathbf{v}_i, (\mathbf{b}_i, B_{-i}))$ for arbitrary misreport \mathbf{b}_i . Furthermore, the auction mechanism needs to be *individually rational (IR)*, ensuring that truthful bidding results in a non-negative utility for each bidder, that is, $u_i(\mathbf{v}_i, (\mathbf{v}_i, B_{-i})) \geq 0$.

Affine Maximizer Auction (AMA) AMAs [Roberts, 1979] is a generalized version of VCG auctions [Vickrey, 1961] and inherently ensures DSIC and IR. A (deterministic) AMA contains positive weights $w_i \in \mathbb{R}_+$ for each bidder and boosts $\lambda(A) \in \mathbb{R}$ for each candidate allocation $A \in \mathcal{A}$, where \mathcal{A} is the set of all the $(n+1)^m$ deterministic allocations. Given bids B , an AMA of parameters $(\mathbf{w}, \boldsymbol{\lambda})$ selects the allocation A^* that maximizes the affine welfare (with an arbitrary tie-breaking rule):

$$A^* = g(B; \mathbf{w}, \boldsymbol{\lambda}) := \operatorname{argmax}_{A \in \mathcal{A}} \sum_{i=1}^n w_i v_i(A) + \lambda(A), \quad (1)$$

and each bidder i pays for her normalized negative affine welfare impact on other bidders:

$$p_i(B; \mathbf{w}, \boldsymbol{\lambda}) = \frac{1}{w_i} \max_{A \in \mathcal{A}} \left(\sum_{j \neq i} w_j b_j(A) + \lambda(A) \right) - \frac{1}{w_i} \left(\sum_{j \neq i} w_j b_j(A^*) + \lambda(A^*) \right). \quad (2)$$

Virtual Valuations Combinatorial Auction (VVCA) VVCAs [Likhodedov et al., 2005] is a subset of AMAs, distinguishing itself by decomposing the boost variable of AMAs into n parts, one for each bidder. Formally, a VVCA boosts per bidder-bundle pair as

$$\lambda(A) = \sum_{i=1}^n \lambda_i(A_i). \quad (\text{VVCA})$$

This decomposition results in a reduction of VVCA parameters from $O((n+1)^m)$ to $O(n \times 2^m)$, aligning with the same order as the input valuation V .

4 Methodology

In this section, we outline the methodology of ZFO-VVCA, as depicted in [Figure 1](#). We begin by formalizing our problem of automated mechanism design for deterministic Virtual Valuations Combinatorial Auctions (VVCAs). Next, we introduce the dynamic programming algorithm for computing the auction results of VVCAs and explain how we optimize the VVCA parameters using objective decomposition.

4.1 Problem Formulation

We aim to discover a high-revenue deterministic auction mechanism that satisfies both DSIC and IR for a sealed-bid auction with n bidders and m items. Since there is currently no known characterization of a DSIC multi-item combinatorial auction [[Dütting et al., 2023](#)], a common strategy is to limit the auction class to AMAs [[Likhodedov et al., 2005](#), [Sandholm and Likhodedov, 2015](#), [Curry et al., 2023](#), [Duan et al., 2023](#)]. AMAs are inherently DSIC and IR, encompassing a broad class of mechanisms [[Lavi et al., 2003](#)]. However, the boost parameters λ are defined across the entire candidate allocations, resulting in $O((n+1)^m)$ parameters. To address the scalability challenges stemming from the parameter space of AMAs, we further constrain the auction class to be (deterministic) Virtual Valuations Combinatorial Auctions (VVCAs). Based on this constraint, we can formalize the auction design problem as the following optimization problem:

$$\max_{\mathbf{w} \in \mathbb{R}_+^n, \lambda \in \mathbb{R}^{n \times 2^m}} R_D(\mathbf{w}, \lambda) := \mathbb{E}_{V \sim D} \left[R(V, \mathbf{w}, \lambda) := \sum_{i=1}^n p_i(V; \mathbf{w}, \lambda) \right], \quad (3)$$

where we define $R(V, \mathbf{w}, \lambda)$ as the revenue of valuation profile V under VVCA parameters \mathbf{w} and λ , which can be further derived as:

$$R(V, \mathbf{w}, \lambda) = \overbrace{\sum_{i=1}^n v_i(g(V; \mathbf{w}, \lambda))}^{Z(V, \mathbf{w}, \lambda)} + \underbrace{\sum_{i=1}^n \frac{1}{w_i} \max_{A \in \mathcal{A}} \left(\sum_{j \neq i} w_j v_j(A) + \sum_{k=1}^n \lambda_k(A_k) \right) - \sum_{i=1}^n \frac{1}{w_i} \max_{A \in \mathcal{A}} \left(\sum_{j=1}^n w_j v_j(A) + \lambda_j(A_j) \right)}_{F(V, \mathbf{w}, \lambda)}, \quad (4)$$

where we denote $Z(V, \mathbf{w}, \lambda)$ and $F(V, \mathbf{w}, \lambda)$ as the two components of $R(V, \mathbf{w}, \lambda)$.

4.2 Winning Allocation Determination

As shown in [Equation \(4\)](#), computing $R(V, \mathbf{w}, \lambda)$ requires finding the winning allocation $g(V; \mathbf{w}, \lambda)$ and the allocation that maximizes the affine welfare for each bidder $i \in [n]$, which can be viewed as the allocation maximizing the valuation profile $(\mathbf{0}, V_{-i})$. Therefore, we need to develop an algorithm to compute the winning allocation for an arbitrary given valuation profile.

The winning allocation determination of a VVCA is NP-Hard [[Likhodedov et al., 2005](#)]. To address this challenge as efficiently as possible, we propose a parallelizable dynamic programming algorithm for computing the winning allocation of VVCAs. Firstly, we denote $\text{MAW}(i, \mathcal{S})$ as the Maximum Affine Welfare if we allocate all items in bundle $\mathcal{S} \in 2^m$ to the first i bidders, and we use $\text{AB}(i, \mathcal{S})$ to record the Allocated Bundle of bidder i . We initialize $\text{MAW}(1, \mathcal{S}) = w_1 v_1(\mathcal{S}) + \lambda_1(\mathcal{S})$ and $\text{AB}(1, \mathcal{S}) = \mathcal{S}$, and compute $\text{MAW}(i, \mathcal{S})$ and $\text{AB}(i, \mathcal{S})$ for $i = 2, 3, \dots, n$ and $\mathcal{S} \in 2^m$ iteratively. The computation of $\text{MAW}(i, \mathcal{S})$ and $\text{AB}(i, \mathcal{S})$ involves enumerating all subsets of \mathcal{S} as the allocated bundle to bidder i , which are given by:

$$\begin{aligned} \text{MAW}(i, \mathcal{S}) &= \max_{\mathcal{B} \subseteq \mathcal{S}} \text{MAW}(i-1, \mathcal{S} \setminus \mathcal{B}) + w_i v_i(\mathcal{B}) + \lambda_i(\mathcal{B}), \\ \text{AB}(i, \mathcal{S}) &= \arg \max_{\mathcal{B} \subseteq \mathcal{S}} \text{MAW}(i-1, \mathcal{S} \setminus \mathcal{B}) + w_i v_i(\mathcal{B}) + \lambda_i(\mathcal{B}), \end{aligned} \quad (5)$$

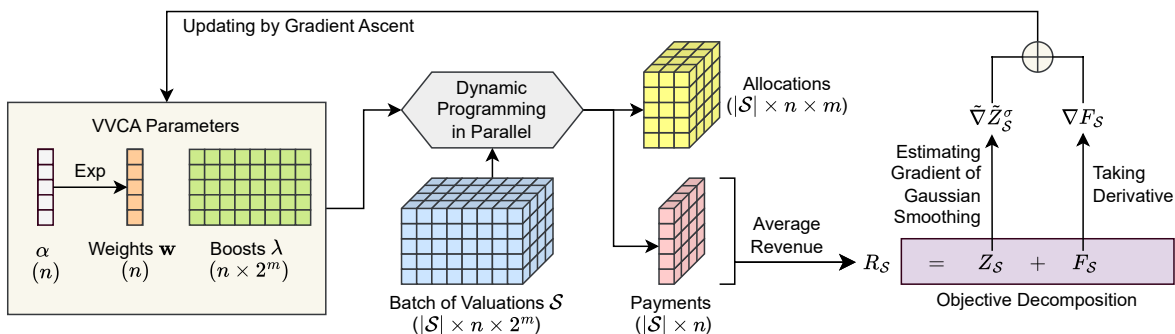


Figure 1: Overview of OD-VVCA for automated design of deterministic auctions. We constrain the mechanism to VVCAs with $n + n \times 2^m$ parameters, introducing $\alpha \in \mathbb{R}^n$ such that $w = e^\alpha \in \mathbb{R}_+^n$ to accommodate the positive range of w . A parallelizable dynamic programming algorithm is employed to compute the allocations and payments for a batch of valuations. Afterward, the average revenue objective is decomposed into two components, and their gradients are estimated or computed directly. By integrating these gradients, we update the VVCA parameters through gradient ascent.

which can be computed in parallel for all subsets \mathcal{B} using vector operations (see [Appendix A](#) for details). Finally, to obtain the winning allocation, we define $\mathcal{S}_n := \operatorname{argmax}_{\mathcal{S} \subseteq [m]} \operatorname{MAW}(n, \mathcal{S})$ as the set of all allocated items in the affine welfare-maximizing allocation, and iteratively determine the allocated bundle $\operatorname{AB}(i, \mathcal{S}_i)$ for bidder $i = n, n-1, \dots, 1$, updating $\mathcal{S}_{i-1} := \mathcal{S}_i - \operatorname{AB}(i, \mathcal{S}_i)$.

The pseudocode of the entire DP algorithm is provided in [Appendix A](#), where we also prove that the time complexity and space complexity of the DP algorithm are $O(n3^m)$ and $O(n2^m)$, respectively. Notably, the input valuation profile is already $O(n2^m)$, demonstrating the efficiency of our dynamic programming algorithm. Furthermore, as we discussed, the computation of [Equation \(5\)](#) can be performed using vector operations. Therefore, when solving the DP for a batch of valuations, we can further accelerate the computation through matrix operations, which can be parallelized using GPUs.

Based on the DP algorithm, we can efficiently compute $R(V, w, \lambda)$ as described in [Equation \(4\)](#). The computation takes $n + 1$ DPs: one to solve the winning allocation for valuation profile V , and n additional DPs to solve for the valuation profile $(0, V_{-i})$ for each bidder $i \in [n]$.

4.3 Optimization

To optimize the VVCA parameters w and λ in [Equation \(3\)](#), we first introduce $\alpha \in \mathbb{R}^n$ as the logarithm of w (such that $w = e^\alpha \in \mathbb{R}_+^n$) and optimize α instead to handle the positive range of w . Then we optimize the empirical revenue, which is defined as:

$$R_S(w = e^\alpha, \lambda) := \frac{1}{|\mathcal{S}|} \sum_{V \in \mathcal{S}} R(V, e^\alpha, \lambda) = \underbrace{\frac{1}{|\mathcal{S}|} \sum_{V \in \mathcal{S}} Z(V, e^\alpha, \lambda)}_{Z_S(e^\alpha, \lambda)} + \underbrace{\frac{1}{|\mathcal{S}|} \sum_{V \in \mathcal{S}} F(V, e^\alpha, \lambda)}_{F_S(e^\alpha, \lambda)}, \quad (6)$$

where \mathcal{S} is a dataset of valuations sampled i.i.d. from D . However, $R_S(e^\alpha, \lambda)$ is non-differentiable with respect to α and λ , since the computation of $R(V, e^\alpha, \lambda)$ involves finding the winning allocation from all deterministic candidate allocations and computing the social welfare of the winning allocation (i.e., $Z(V, e^\alpha, \lambda)$ in [Equation \(4\)](#)). Therefore, we decompose it into two parts: $F_S(e^\alpha, \lambda)$ and $Z_S(e^\alpha, \lambda)$, and optimize them separately.

The optimization of $F_S(e^\alpha, \lambda)$ is straightforward since it is a continuous and piece-wise non-constant linear function with respect to e^α and λ . Thus, we can easily optimize $F_S(e^\alpha, \lambda)$ through its gradient $\nabla F_S(e^\alpha, \lambda)$, where the gradient of the maximum function can be estimated similarly to the ReLU function.

However, optimizing $Z_S(e^\alpha, \lambda)$ is more challenging. This is because $Z_S(e^\alpha, \lambda)$ is a discontinuous, piece-wise constant function. Its derivatives at differentiable points are always 0, and it undergoes sudden changes at the non-differentiable discontinuous points, making it not feasible to optimize $Z_S(e^\alpha, \lambda)$ using its own gradient. To address this issue, similar to [Bichler et al. \[2021\]](#), we optimize

$Z_S(e^\alpha, \lambda)$ using Gaussian smoothing techniques. Specifically, we optimize the Gaussian smoothing approximation of $Z_S(e^\alpha, \lambda)$, which is defined as:

$$\tilde{Z}_S^\sigma(e^\alpha, \lambda) := \mathbb{E}_{\epsilon \sim N(0,1)^n, \delta \sim N(0,1)^{n \times 2^m}} [Z_S(e^{\alpha+\sigma\epsilon}, \lambda + \sigma\delta)],$$

where $\sigma > 0$ and $N(0, 1)$ is the standard normal distribution. Clearly, as $\sigma \rightarrow 0$, $\tilde{Z}_S^\sigma(e^\alpha, \lambda)$ approaches $Z_S(e^\alpha, \lambda)$. As for the differentiability property of $\tilde{Z}_S^\sigma(e^\alpha, \lambda)$, we have the following proposition:

Proposition 4.1. $\tilde{Z}_S^\sigma(e^\alpha, \lambda)$ is continuous and differentiable with derivatives:

$$\begin{aligned} \nabla_\alpha \tilde{Z}_S^\sigma(e^\alpha, \lambda) &= \mathbb{E}_{\epsilon \sim N(0,1)^n, \delta \sim N(0,1)^{n \times 2^m}} \left[\frac{Z_S(e^{\alpha+\sigma\epsilon}, \lambda + \sigma\delta) - Z_S(e^\alpha, \lambda)}{\sigma} \epsilon \right] \\ \nabla_\lambda \tilde{Z}_S^\sigma(e^\alpha, \lambda) &= \mathbb{E}_{\epsilon \sim N(0,1)^n, \delta \sim N(0,1)^{n \times 2^m}} \left[\frac{Z_S(e^{\alpha+\sigma\epsilon}, \lambda + \sigma\delta) - Z_S(e^\alpha, \lambda)}{\sigma} \delta \right]. \end{aligned}$$

According to [Proposition 4.1](#), we can unbiasedly estimate the gradient of $\tilde{Z}_S^\sigma(e^\alpha, \lambda)$ by Monte Carlo sampling, which is done by computing the average of numerical differentiations in n_r random directions generated by Gaussian sampling:

$$\begin{aligned} \nabla_\alpha \tilde{Z}_S(e^\alpha, \lambda) &\approx \tilde{\nabla}_\alpha \tilde{Z}_S(e^\alpha, \lambda) = \frac{1}{n_r} \sum_{i=1}^{n_r} \frac{1}{\sigma} (Z_S(e^{\alpha+\sigma\epsilon_i}, \lambda + \sigma\delta_i) - Z_S(e^\alpha, \lambda)) \epsilon_i, \\ \nabla_\lambda \tilde{Z}_S(e^\alpha, \lambda) &\approx \tilde{\nabla}_\lambda \tilde{Z}_S(e^\alpha, \lambda) = \frac{1}{n_r} \sum_{i=1}^{n_r} \frac{1}{\sigma} (Z_S(e^{\alpha+\sigma\epsilon_i}, \lambda + \sigma\delta_i) - Z_S(e^\alpha, \lambda)) \delta_i, \end{aligned}$$

where $\epsilon_i \sim N(0, 1)^n$, and $\delta_i \sim N(0, 1)^{n \times 2^m}$. It takes totally n_r additional DPs to get the estimated gradient $\tilde{\nabla} Z_S(e^\alpha, \lambda)$, based on which we can optimize $\tilde{Z}_S^\sigma(e^\alpha, \lambda)$ through gradient ascent. This approach offers an approximate method for optimizing $Z_S(e^\alpha, \lambda)$.

Remark 4.2. It is also feasible to optimize $R_S(e^\alpha, \lambda)$ using the same Gaussian smoothing technique as $Z_S(e^\alpha, \lambda)$. However, this approach would require $(n+1)n_r$ additional DPs to compute the estimated gradient. In comparison, our objective decomposition reduces the number of additional DPs to n_r , enhancing efficiency significantly.

5 Experiments

In this section, we present empirical experiments to evaluate the effectiveness of ZFO-VVCA. These experiments are conducted on a Linux machine equipped with 4 NVIDIA Graphics Processing Units (GPUs), each with a memory size of 11GB. Each result is averaged across 5 distinct runs. The standard deviation of ZFO-VVCA across all these runs is below 1%.

5.1 Setup

Auction Settings We consider a variety of valuation distributions, including both symmetric and asymmetric, as well as additive and combinatorial types. They are listed as follows:

- (A) (Symmetric Uniform) For all bidder i and item j , the valuation v_{ij} is sampled from $U[0, 1]$. The valuation is additive, that is, for all item bundle S and bidder i , $v_i(S) = \sum_{j \in S} v_{ij}$. This setting is widely used in previous researches [[Sandholm and Likhodedov, 2015](#), [Dütting et al., 2019](#), [Curry et al., 2023](#)].
- (B) (Asymmetric Uniform) For all bidder i and item j , the valuation v_{ij} is sampled from $U[0, i]$. The valuation is additive but asymmetric for bidders.
- (C) (Lognormal) For all bidder i and item j , the valuation v_{ij} is sampled from $\text{Lognormal}(0, 1/i^2)$. The valuation is additive but asymmetric for bidders.
- (D) (Combinatorial) For all bidder i and item j , the valuation v_{ij} is sampled from $U[1, 2]$. For item bundle $S \subseteq [m]$ and bidder i , the valuation $v_i(S) = \sum_{j \in S} v_{ij} + \epsilon_{iS}$, where ϵ_{iS} is sampled from $U[-|S|/2, |S|/2]$. This setting is also used in [Sandholm and Likhodedov \[2015\]](#).

Table 1: The revenue results in both small and large settings. For each setting, the highest revenue among all methods is **bolded**, and the highest revenue among all deterministic methods (the methods except for Lottery AMA and AMenuNet) is underlined. It is important to note that we do not report the results of Item-Myerson, Lottery AMA, and AMenuNet for setting (D). This is because Item-Myerson is not DSIC in a non-additive scenario, and Lottery AMA and AMenuNet are not applicable for combinatorial valuations.

(a) Revenue results in small-scale settings.

Method	Symmetric					Asymmetric				
	2×2(A)	2×5(A)	3×10(A)	2×2(D)	3×10(D)	5×3(B)	3×10(B)	2×5(C)	5×3(C)	3×10(C)
Lottery AMA	0.8680	2.2354	5.3450	-	-	6.5904	11.9814	5.7001	4.0195	12.9863
AMenuNet	0.8618	2.2768	5.5986	-	-	6.7743	12.3419	5.6512	4.1919	13.6094
VCG	0.6678	1.6691	5.0032	2.4576	15.6305	6.0470	8.9098	3.8711	3.7249	10.6495
Item-Myerson	<u>0.8330</u>	2.0755	5.3141	-	-	5.3909	8.9110	4.4380	3.6918	9.3740
BBBVCA	0.7781	2.2576	5.7647	2.6111	16.3504	6.6118	10.5134	4.8174	4.1879	11.4605
FO-VVCA	0.7836	<u>2.2638</u>	5.7876	2.6205	16.3786	6.8783	11.8093	5.5536	4.1906	13.0144
ZFO-VVCA	0.8284	2.2632	5.8230	2.6802	16.3675	7.0344	12.5497	<u>5.6682</u>	4.3289	13.6223

(b) Revenue results in large-scale settings.

Method	Symmetric				Asymmetric					
	5×10(A)	10×5(A)	5×10(D)	10×5(D)	5×10(B)	10×5(B)	30×5(B)	5×10(C)	10×5(C)	30×5(C)
Lottery AMA	5.5435	3.0210	-	-	21.4092	24.3684	74.1259	13.0961	6.1878	4.8812
AMenuNet	6.5210	3.8156	-	-	21.7912	27.4230	88.2373	13.6266	7.0347	6.1055
VCG	6.6690	4.0887	17.2580	9.4405	20.1567	26.7979	105.4290	12.4163	6.5472	6.6054
Item-Myerson	6.7132	4.0868	-	-	17.9697	24.7287	102.1878	12.3060	7.4868	7.6173
BBBVCA	6.9765	4.1038	17.4657	9.4356	22.4459	28.2620	107.5630	14.4585	7.4899	7.4989
FO-VVCA	6.9904	<u>4.1107</u>	17.5026	9.4397	23.1474	28.4363	107.8873	14.6641	7.2678	7.0965
ZFO-VVCA	6.9848	4.0830	17.4614	9.4388	24.4301	28.9711	108.2780	<u>14.8071</u>	7.5882	7.6446

Baselines We compare OD-VVCA against both randomized and deterministic methods. The randomized methods include:

1. *Lottery AMA* [Curry et al., 2023], a randomized AMA-based approach that directly sets the candidate allocations, bidder weights, and boost variables as all the learnable weights.
2. *AMenuNet* [Duan et al., 2023], similar to Lottery AMA, but uses a transformer-based architecture to optimize the parameters of AMA, hence more powerful and applicable to general contextual auctions.

Note that we ignore the regret-based methods [Dütting et al., 2019] since they are not strictly IC, and thus not directly comparable to ZFO-VVCA. The deterministic methods include:

1. VCG [Vickrey, 1961], which is the most classical special case of VVCA.
2. Item-Myerson [Myerson, 1981], a strong baseline that independently applies Myerson auction with respect to each item.
3. BBBVCA [Likhodedov et al., 2005, Sandholm and Likhodedov, 2015], the pioneering work of optimizing VVCA parameters, which minimizes the revenue loss for each bidder-bundle by gradient descent. We use the same dynamic programming algorithm as ZFO-VVCA to compute the winning allocation.
4. FO-VVCA, an ablated version of ZFO-VVCA which only optimizes $F_S(e^\alpha, \lambda)$.

Hyperparameters and Implementation For ZFO-VVCA, we select the number of random directions n_r from $\{8, 16, 32\}$ and the standard deviation σ from $\{0.01, 0.003, 0.001\}$. The training starts at classic VCG, i.e., $\mathbf{w} = 1$ and $\lambda = 0$. For Lottery AMA and AMenuNet, since the candidate allocation set cannot be arbitrarily large due to the constraint of computational resources, we select the candidate size from $\{32, 128, 1024, 4096\}$ to balance their performance and computational feasibility. Further implementation details of ZFO-VVCA and baseline methods can be found in Appendix C.

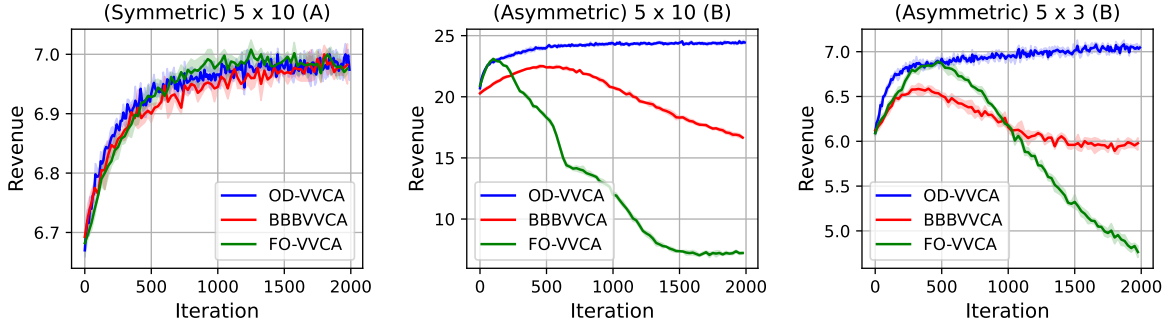


Figure 2: Training curves for OD-VVCA, BBBVVCA, and FO-VVCA under 5×10 (A), 5×10 (B) and 5×3 (B). The plots depict average results across 5 runs and the 95%

5.2 Revenue Experiments

The results of revenue experiments are presented in Table 1, where we use the notation $n \times m(X)$ to denote an auction with n bidders and m items of setting (X). All the machine learning-based methods take comparable training time, which we discuss in Appendix D.

Among the deterministic baselines, ZFO-VVCA outperforms them in most settings, especially in large-scale asymmetric scenarios. Specifically, the comparison between ZFO-VVCA and VCG demonstrates that integrating affine parameters into VCG significantly enhances revenue, and the comparison between ZFO-VVCA and Item-Myerson indicates the strong revenue performance of ZFO-VVCA. OD-VVCA is also distinctly advantageous over BBBVVCA, which optimizes VVCA parameters under a fixed winning allocation and overlooks the impact of these parameters on allocation outcomes. Additionally, ZFO-VVCA consistently outperforms FO-VVCA across various asymmetric and most symmetric settings, underscoring the efficacy of the Gaussian smoothing technique to optimize $Z_S(e^\alpha, \lambda)$.

Among the randomized baselines, Lottery AMA and AMenuNet both demonstrate commendable performance in smaller settings. However, in larger settings, as shown in Table 1, ZFO-VVCA consistently outperforms these two randomized AMA methods. This outcome suggests that within the constraint of computational resource limitations, ZFO-VVCA is more effective than Lottery AMA and AMenuNet, particularly in handling larger settings.

5.3 Case Study

To further illustrate the advantages of ZFO-VVCA over BBBVVCA and FO-VVCA, we present the revenue trajectories of them during training in symmetric (5×10 (A)) and asymmetric (5×10 (B) and 5×3 (B)) scenarios in Figure 2. We can see that while all three methods converge to similar revenue in the symmetric 5×10 (A) scenario, the revenue of BBBVVCA and FO-VVCA declines significantly in the two asymmetric settings. The instability of BBBVVCA highlights the drawbacks of neglecting the influence of VVCA parameters on winning allocation. Meanwhile, the comparison between OD-VVCA and OD-VVCA indicates the effectiveness and stability of incorporating the Gaussian smoothing technique in optimizing VVCA parameters.

To visualize the training process of OD-VVCA, we adopt a symmetric simplification for bidders and items in 2×2 ((A)). Specifically, we fix the bidder weights $w_1 = w_2 = 1$ and $\lambda_1(\emptyset) = \lambda_2(\emptyset) = 0$, then we set other boosts as:

$$\lambda_1(\{1\}) = \lambda_2(\{1\}) = \lambda_1(\{2\}) = \lambda_2(\{2\}) = x, \quad \lambda_1(\{1, 2\}) = \lambda_2(\{1, 2\}) = y.$$

Under this simplification, when fixing a dataset of valuation \mathcal{S} , we use $R(x, y)$, $F(x, y)$, and $Z(x, y)$ to denote $R_S(\mathbf{w}, \lambda)$, $F_S(\mathbf{w}, \lambda)$, $Z_S(\mathbf{w}, \lambda)$, respectively. In Figure 3, we illustrate the trajectory of (x, y) concurrently on $R(x, y)$, $F(x, y)$, and $Z(x, y)$. Here, $R(x, y) = F(x, y) + Z(x, y)$ according to Equation (6). The trajectory initiates from a VCG auction (i.e., $x = y = 0$), and converges to an improved solution that balances the values of both $F(x, y)$ and $Z(x, y)$. This outcome underscores the efficacy of our Gaussian smoothing technique to optimize $Z(x, y)$.

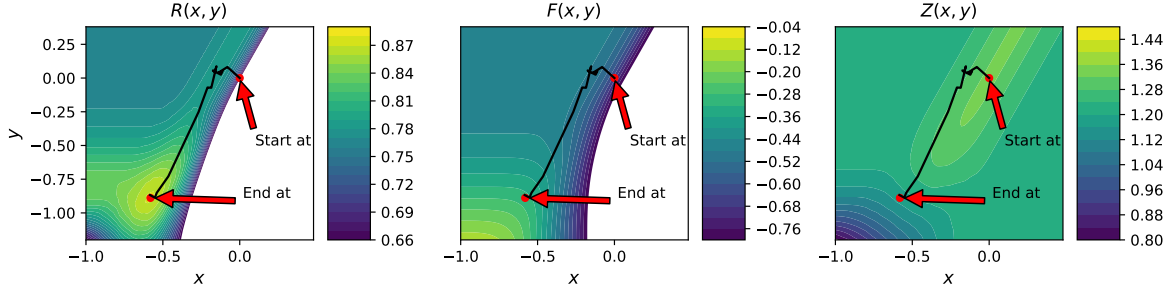


Figure 3: Training dynamics of OD-VVCA over 2000 iterations in 2×2 ((A)). The trajectory of (x, y) is simultaneously plotted on $R(x, y)$, $F(x, y)$, and $Z(x, y)$. The trajectory converges at a point balancing the values of both $F(x, y)$ and $Z(x, y)$, illustrating the effectiveness of optimizing $R(x, y)$ through objective decomposition.

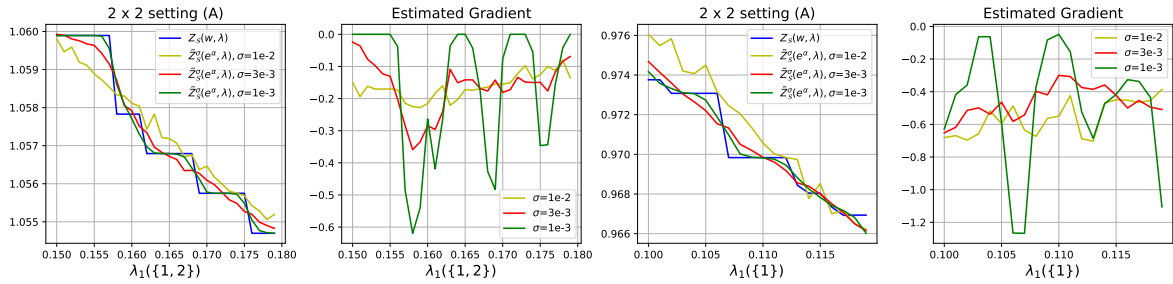


Figure 4: Visualization of $Z_S(e^\alpha, \lambda)$, $\tilde{Z}_S^\sigma(e^\alpha, \lambda)$, and the corresponding estimated gradient $\tilde{\nabla} \tilde{Z}_S^\sigma(e^\alpha, \lambda)$ in 2×2 (A) with respect to one parameter.

To further illustrate the impact of the Gaussian smoothing technique in OD-VVCA, we explore a 2×2 scenario ((A)), adjusting only one of the boost variables λ while maintaining the remaining VVCA parameters fixed. We plot $Z_S(\mathbf{w}, \lambda)$ alongside the computed $\tilde{Z}_S^\sigma(\mathbf{w}, \lambda)$ for three distinct σ values in Figure 4. The figure shows that $Z_S(\mathbf{w}, \lambda)$ experiences non-differentiability at several points. The Gaussian smoothing technique addresses this by smoothing $Z_S(\mathbf{w}, \lambda)$, with varying smoothness achieved by different σ values. Specifically, a smaller σ provides a closer approximation of $\tilde{Z}_S^\sigma(\mathbf{w}, \lambda)$ to $Z_S(\mathbf{w}, \lambda)$, and a larger σ results in a less precise approximation but more effectively captures the general trend with a flatter gradient. Though these insights emphasize the criticality of careful parameter selection in OD-VVCA, they do not necessarily imply difficulty in tuning the hyperparameters. In practice, our experiments indicate that σ values within $\{0.01, 0.003, 0.001\}$ are generally well-suited for most scenarios.

6 Conclusion and Future Work

In this paper, we introduce OD-VVCA, an objective decomposition approach for designing deterministic Virtual Valuation Combinatorial Auctions (VVCAs). Our method employs a parallelizable dynamic programming algorithm to compute the winning allocation and revenue in a VVCA efficiently. Subsequently, we decompose the objective function of revenue into continuous and discontinuous components. The continuous portion can be directly optimized by taking derivatives. For the discontinuous part, we use Monte Carlo estimation to approximate the gradient of its Gaussian-smoothed version. Finally, we demonstrate the efficacy, stability, and scalability of OD-VVCA in various auction settings through experimental results.

As for future work, while OD-VVCA is tailored for general combinatorial auctions, exploring its adaptation for industrial applications presents an intriguing avenue. Additionally, given that the Gaussian smoothing technique requires extra iterations to approximate the gradient via Monte Carlo

sampling, it would be valuable to investigate more efficient methods for gradient approximation.

References

- M-F Balcan, Siddharth Prasad, and Tuomas Sandholm. Learning within an instance for designing high-revenue combinatorial auctions. In *IJCAI Annual Conference*, 2021.
- Maria-Florina Balcan, Tuomas Sandholm, and Ellen Vitercik. A general theory of sample complexity for multi-item profit maximization. In *Proceedings of the 2018 ACM Conference on Economics and Computation*, pages 173–174, 2018.
- Maria-Florina Balcan, Tuomas Sandholm, and Ellen Vitercik. Generalization guarantees for multi-item profit maximization: Pricing, auctions, and randomized mechanisms. *Operations Research*, 2023.
- Maria-Florina F Balcan, Tuomas Sandholm, and Ellen Vitercik. Sample complexity of automated mechanism design. *Advances in Neural Information Processing Systems*, 29, 2016.
- Martin Bichler, Maximilian Fichtl, Stefan Heidekrüger, Nils Kohring, and Paul Sutterer. Learning equilibria in symmetric auction games using artificial neural networks. *Nature machine intelligence*, 3(8):687–695, 2021.
- Michael Curry, Ping-Yeh Chiang, Tom Goldstein, and John Dickerson. Certifying strategyproof auction networks. *Advances in Neural Information Processing Systems*, 33:4987–4998, 2020.
- Michael J Curry, Uro Lyi, Tom Goldstein, and John P Dickerson. Learning revenue-maximizing auctions with differentiable matching. In *International Conference on Artificial Intelligence and Statistics*, pages 6062–6073. PMLR, 2022.
- Michael J. Curry, Tuomas Sandholm, and John P. Dickerson. Differentiable economics for randomized affine maximizer auctions. In *Proceedings of the Thirty-Second International Joint Conference on Artificial Intelligence, IJCAI 2023, 19th-25th August 2023, Macao, SAR, China*, pages 2633–2641. ijcai.org, 2023. doi: 10.24963/ijcai.2023/293. URL <https://doi.org/10.24963/ijcai.2023/293>.
- Zhijian Duan, Jingwu Tang, Yutong Yin, Zhe Feng, Xiang Yan, Manzil Zaheer, and Xiaotie Deng. A context-integrated transformer-based neural network for auction design. In *International Conference on Machine Learning*, pages 5609–5626. PMLR, 2022.
- Zhijian Duan, Haoran Sun, Yurong Chen, and Xiaotie Deng. A scalable neural network for DSIC affine maximizer auction design. *Advances in Neural Information Processing Systems*, 36, 2023.
- Paul Dütting, Zhe Feng, Harikrishna Narasimhan, David Parkes, and Sai Srivatsa Ravindranath. Optimal auctions through deep learning. In *International Conference on Machine Learning*, pages 1706–1715. PMLR, 2019.
- Paul Dütting, Zhe Feng, Harikrishna Narasimhan, David C Parkes, and Sai Srivatsa Ravindranath. Optimal auctions through deep learning: Advances in differentiable economics. *Journal of the ACM*, 2023.
- Benjamin Edelman, Michael Ostrovsky, and Michael Schwarz. Internet advertising and the generalized second-price auction: Selling billions of dollars worth of keywords. *American economic review*, 97(1): 242–259, 2007.
- Noah Golowich, Harikrishna Narasimhan, and David C Parkes. Deep learning for multi-facility location mechanism design. In *IJCAI*, pages 261–267, 2018.
- Dmitry Ivanov, Iskander Safulin, Igor Filippov, and Ksenia Balabaeva. Optimal-er auctions through attention. *Advances in Neural Information Processing Systems*, 35:34734–34747, 2022.
- Philippe Jehiel, Moritz Meyer-Ter-Vehn, and Benny Moldovanu. Mixed bundling auctions. *Journal of Economic Theory*, 134(1):494–512, 2007.

- Ron Lavi, Ahuva Mu’Alem, and Noam Nisan. Towards a characterization of truthful combinatorial auctions. In *44th Annual IEEE Symposium on Foundations of Computer Science, 2003. Proceedings.*, pages 574–583. IEEE, 2003.
- Xuejian Li, Ze Wang, Bingqi Zhu, Fei He, Yongkang Wang, and Xingxing Wang. Deep automated mechanism design for integrating ad auction and allocation in feed. *arXiv preprint arXiv:2401.01656*, 2024.
- Anton Likhodedov and Tuomas Sandholm. Methods for boosting revenue in combinatorial auctions. In *AAAI*, pages 232–237, 2004.
- Anton Likhodedov, Tuomas Sandholm, et al. Approximating revenue-maximizing combinatorial auctions. In *AAAI*, volume 5, pages 267–274, 2005.
- Xiangyu Liu, Chuan Yu, Zhilin Zhang, Zhenzhe Zheng, Yu Rong, Hongtao Lv, Da Huo, Yiqing Wang, Dagui Chen, Jian Xu, et al. Neural auction: End-to-end learning of auction mechanisms for e-commerce advertising. In *Proceedings of the 27th ACM SIGKDD Conference on Knowledge Discovery & Data Mining*, pages 3354–3364, 2021.
- Roger B Myerson. Optimal auction design. *Mathematics of operations research*, 6(1):58–73, 1981.
- Neehar Peri, Michael Curry, Samuel Dooley, and John Dickerson. Preferencenet: Encoding human preferences in auction design with deep learning. *Advances in Neural Information Processing Systems*, 34:17532–17542, 2021.
- Jad Rahme, Samy Jelassi, Joan Bruna, and S Matthew Weinberg. A permutation-equivariant neural network architecture for auction design. In *Proceedings of the AAAI Conference on Artificial Intelligence*, volume 35, pages 5664–5672, 2021a.
- Jad Rahme, Samy Jelassi, and S. Matthew Weinberg. Auction learning as a two-player game. In *International Conference on Learning Representations*, 2021b. URL <https://openreview.net/forum?id=YHdeA06116T>.
- Sai Srivatsa Ravindranath, Zhe Feng, Shira Li, Jonathan Ma, Scott D Kominers, and David C Parkes. Deep learning for two-sided matching. *arXiv preprint arXiv:2107.03427*, 2021.
- Sai Srivatsa Ravindranath, Yanchen Jiang, and David C. Parkes. Data market design through deep learning. In *Thirty-seventh Conference on Neural Information Processing Systems*, 2023. URL <https://openreview.net/forum?id=sgCrNM0uXp>.
- Kevin Roberts. The characterization of implementable choice rules. *Aggregation and revelation of preferences*, 12(2):321–348, 1979.
- Michael H Rothkopf, Aleksandar Pekeč, and Ronald M Harstad. Computationally manageable combinatorial auctions. *Management science*, 44(8):1131–1147, 1998.
- Tuomas Sandholm and Anton Likhodedov. Automated design of revenue-maximizing combinatorial auctions. *Operations Research*, 63(5):1000–1025, 2015.
- Pingzhong Tang and Tuomas Sandholm. Mixed-bundling auctions with reserve prices. In *AAMAS*, pages 729–736, 2012.
- William Vickrey. Counterspeculation, auctions, and competitive sealed tenders. *The Journal of finance*, 16(1):8–37, 1961.

A About the Winning Allocation Deterministic Dynamic Programming

In this section, we further discuss our proposed dynamic programming (DP) algorithm for winning allocation determination in [Section 4.2](#).

A.1 The Parallel implementation of the DP

For a single valuation V , given the bidder i and the item bundle \mathcal{S} , we can compute $\text{MAW}(i, \mathcal{S})$ and $\text{AB}(i, \mathcal{S})$ according to [Equation \(5\)](#) using vector operations, which can be parallelized by the GPU. Firstly, for all item bundle $\mathcal{S} \subseteq [m]$, we denote the set of all subsets of \mathcal{S} as $\overrightarrow{\mathcal{B}(\mathcal{S})} := (\mathcal{B})_{\mathcal{B} \subseteq \mathcal{S}}$, which is a $2^{|\mathcal{S}|}$ -dimensional vector. On top of that, we can compute the intermediate result $\text{Int}(i, \mathcal{S}, \overrightarrow{\mathcal{B}(\mathcal{S})}) = (\text{Int}(i, \mathcal{S}, \mathcal{B}))_{\mathcal{B} \in \overrightarrow{\mathcal{B}(\mathcal{S})}}$ by vector operations:

$$\text{Int}(i, \mathcal{S}, \overrightarrow{\mathcal{B}(\mathcal{S})}) = \text{MAW}(i-1, \mathcal{S} - \overrightarrow{\mathcal{B}(\mathcal{S})}) + w_i v_i(\overrightarrow{\mathcal{B}(\mathcal{S})}) + \lambda_i(\overrightarrow{\mathcal{B}(\mathcal{S})})$$

Subsequently, we can obtain $\text{MAW}(i, \mathcal{S})$ and $\text{AB}(i, \mathcal{S})$ by computing the maximum element of the vector $\text{Int}(i, \mathcal{S}, \overrightarrow{\mathcal{B}(\mathcal{S})})$:

$$\text{MAW}(i, \mathcal{S}) = \max_{\mathcal{B} \in \overrightarrow{\mathcal{B}(\mathcal{S})}} \text{Int}(i, \mathcal{S}, \mathcal{B}), \quad \text{AB}(i, \mathcal{S}) = \operatorname{argmax}_{\mathcal{B} \in \overrightarrow{\mathcal{B}(\mathcal{S})}} \text{Int}(i, \mathcal{S}, \mathcal{B})$$

It is evident that all these operations are vector-based.

In summary, we provide the pseudocode of the parallel DP implementation for a single valuation in [Algorithm 1](#). For the valuations in a minibatch $\mathcal{S} = V^1, V^2, \dots, V^{\mathcal{S}}$, we can compute all the DP computations through matrix operations. The reason is that, as discussed above, the DP computation for a single valuation involves vector operations. Thus, the computation for all valuations can be executed using matrix operations.

Algorithm 1 Winning Allocation Determination by Dynamic Programming

- 1: **Input:** Valuation V , VVCA parameters $\mathbf{w} \in \mathbb{R}_+^n$ and $\boldsymbol{\lambda} \in \mathbb{R}^{n2^m}$.
 - 2: **Output:** Maximum affine welfare MAW^* and the corresponding allocation A^* .
 - 3: **for** $\mathcal{S} \subseteq [m]$ **do**
 - 4: Initialize $\text{MAW}(1, \mathcal{S}) \leftarrow w_1 v_1(\mathcal{S}) + \lambda_1(\mathcal{S})$.
 - 5: Initialize $\text{AB}(1, \mathcal{S}) \leftarrow \mathcal{S}$.
 - 6: Initialize $\overrightarrow{\mathcal{B}(\mathcal{S})} \leftarrow (\mathcal{B})_{\mathcal{B} \subseteq \mathcal{S}}$.
 - 7: **end for**
 - 8: **for** $i = 2$ **to** n **do**
 - 9: **for** $\mathcal{S} \subseteq [m]$ **do**
 - 10: Compute the intermediate result:
 $\text{Int}(i, \mathcal{S}, \overrightarrow{\mathcal{B}(\mathcal{S})}) = \text{MAW}(i-1, \mathcal{S} - \overrightarrow{\mathcal{B}(\mathcal{S})}) + w_i v_i(\overrightarrow{\mathcal{B}(\mathcal{S})}) + \lambda_i(\overrightarrow{\mathcal{B}(\mathcal{S})})$
 - 11: Compute the maximum affine welfare when allocating \mathcal{S} to the previous i bidders:
 $\text{MAW}(i, \mathcal{S}) = \max_{\mathcal{B} \in \overrightarrow{\mathcal{B}(\mathcal{S})}} \text{Int}(i, \mathcal{S}, \mathcal{B})$
 - 12: Record the allocated bundle of bidder i :
 $\text{AB}(i, \mathcal{S}) \leftarrow \operatorname{argmax}_{\mathcal{B} \in \overrightarrow{\mathcal{B}(\mathcal{S})}} \text{Int}(i, \mathcal{S}, \mathcal{B})$
 - 13: **end for**
 - 14: **end for**
 - 15: $\mathcal{S}_n \leftarrow \operatorname{argmax}_{\mathcal{S} \subseteq [m]} \text{MAW}(n, \mathcal{S})$.
 - 16: **for** $i = n$ **to** 1 **do**
 - 17: $A_i^* \leftarrow \text{AB}(i, \mathcal{S}_i)$, the allocated bundle of bidder i .
 - 18: $\mathcal{S}_{i-1} \leftarrow \mathcal{S}_i - A_i^*$
 - 19: **end for**
 - 20: **return** Winning Allocation $A^* = (A_1^*, A_2^*, \dots, A_n^*)$
-

A.2 Time and Space Complexity Analysis

Proposition A.1. *The time and space complexity of the winning allocation deterministic dynamic programming are $O(n3m)$ and $O(n2m)$, respectively.*

Proof. Clearly, the initialization loop and the final loop involve 2^m and n enumerations, respectively. In the dynamic programming loop, for each bidder $i \in [2, n]$ and bundle $|\mathcal{S}| = k$, we need to enumerate all 2^k subsets of \mathcal{S} . Consequently, the total number of enumerations for bidder i is given by $\sum_{k=0}^m \binom{m}{k} 2^k = (2+1)^m = 3^m$. Since the computation during each enumeration is $O(1)$, the overall time complexity is $O(2^m) + O((n-1)3^m) + O(n) = O(n3^m)$.

Regarding space complexity, apart from the $O(n2^m)$ needed for input valuations and VVCA parameters, we require an additional $O(n2^m)$ space to store MAW and AB. Notably, there is no need to store MAW'. Therefore, the total space complexity is $O(n2^m)$. \square

B Proof of Proposition 4.1

Proposition 4.1. $\tilde{Z}_S^\sigma(e^\alpha, \lambda)$ is continuous and differentiable with derivatives:

$$\begin{aligned}\nabla_\alpha \tilde{Z}_S^\sigma(e^\alpha, \lambda) &= \mathbb{E}_{\epsilon \sim N(0,1)^n, \delta \sim N(0,1)^{n \times 2^m}} \left[\frac{Z_S(e^{\alpha+\sigma\epsilon}, \lambda + \sigma\delta) - Z_S(e^\alpha, \lambda)}{\sigma} \epsilon \right] \\ \nabla_\lambda \tilde{Z}_S^\sigma(e^\alpha, \lambda) &= \mathbb{E}_{\epsilon \sim N(0,1)^n, \delta \sim N(0,1)^{n \times 2^m}} \left[\frac{Z_S(e^{\alpha+\sigma\epsilon}, \lambda + \sigma\delta) - Z_S(e^\alpha, \lambda)}{\sigma} \delta \right].\end{aligned}$$

To prove Proposition 4.1, we first present a useful lemma:

Lemma B.1. *Let $W : \mathbb{R}^n \rightarrow \mathbb{R}$ be a bounded function such that $\max_{x \in \mathbb{R}^n} |W(x)| \leq M_W$, and denote $\tilde{W}^\sigma := \mathbb{E}_{\mathbf{u} \sim N(0,1)^n} [W(\mathbf{x} + \sigma\mathbf{u})]$ with $\sigma > 0$ as the Gaussian smoothing approximation of W . Then \tilde{W}^σ is differentiable.*

Proof. For any $\mathbf{x} = (x_1, x_2, \dots, x_n)$, without loss of generality, let's examine the differentiability of $\tilde{W}^\sigma(\mathbf{x})$ with respect to x_1 . We define $\mathbf{x}_{-1} = (x_2, x_3, \dots, x_n)$, and for any $\mathbf{u} \in \mathbb{R}^n$, we denote $\mathbf{u}_{-1} = (u_1, \mathbf{u}_{-1})$.

Existence of $\frac{\partial \tilde{W}^\sigma(\mathbf{x})}{\partial x_1}$ We prove the existence of $\frac{\partial \tilde{W}^\sigma(\mathbf{x})}{\partial x_1}$ by deriving according to the definition of partial derivative:

$$\begin{aligned}& \lim_{\Delta x_1 \rightarrow 0} \frac{\tilde{W}^\sigma(x_1 + \Delta x_1, \mathbf{x}_{-1}) - \tilde{W}^\sigma(x_1, \mathbf{x}_{-1})}{\Delta x_1} \\ &= \lim_{\Delta x_1 \rightarrow 0} \frac{\mathbb{E}_{\mathbf{u} \sim N(0, I_n)} [W(x_1 + \Delta x_1 + \sigma u_1, \mathbf{x}_{-1} + \sigma \mathbf{u}_{-1})] - \mathbb{E}_{\mathbf{u} \sim N(0, I_n)} [W(x_1 + \sigma u_1, \mathbf{x}_{-1} + \sigma \mathbf{u}_{-1})]}{\Delta x_1} \\ &= \lim_{\Delta x_1 \rightarrow 0} \frac{\mathbb{E}_{\mathbf{u}' := (u'_1, \mathbf{u}_{-1}) \sim N((\frac{\Delta x_1}{\sigma}, \mathbf{0}_{n-1}), I_n)} [W(x_1 + \sigma u'_1, \mathbf{x}_{-1} + \sigma \mathbf{u}_{-1})] - \mathbb{E}_{\mathbf{u} \sim N(0, I_n)} [W(x_1 + \sigma u_1, \mathbf{x}_{-1} + \sigma \mathbf{u}_{-1})]}{\Delta x_1} \\ &= \lim_{\Delta x_1 \rightarrow 0} \left(\frac{1}{2\pi} \right)^{\frac{n}{2}} \int W(\mathbf{x} + \sigma \mathbf{u}) \frac{\exp(-\frac{1}{2}\|(u_1 - \frac{\Delta x_1}{\sigma}, \mathbf{u}_{-1})\|^2) - \exp(-\frac{1}{2}\|(u_1, \mathbf{u}_{-1})\|^2)}{\Delta x_1} d\mathbf{u} \quad (7) \\ &\stackrel{(a)}{=} \left(\frac{1}{2\pi} \right)^{\frac{n}{2}} \int W(\mathbf{x} + \sigma \mathbf{u}) \frac{u_1}{\sigma} \exp\left(-\frac{1}{2}\|\mathbf{u}\|^2\right) d\mathbf{u} \\ &= \mathbb{E}_{\mathbf{u} \sim N(0, I)} \left[\frac{W(\mathbf{x} + \sigma \mathbf{u})}{\sigma} u_1 \right] \\ &= \mathbb{E}_{\mathbf{u} \sim N(0, I)} \left[\frac{W(\mathbf{x} + \sigma \mathbf{u}) - W(\mathbf{x})}{\sigma} u_1 \right], \quad \text{since } \mathbb{E}_{\mathbf{u} \sim N(0, I)} [W(\mathbf{x}) u_1] = 0,\end{aligned}$$

where (a) in Equation (7) essentially comes from Taylor expansion. To provide its proof in detail, we first define $f(t) := \exp(-\frac{1}{2}\|(t, \mathbf{u}_{-1})\|^2)$. Then we use Taylor expansion of $f(u_1 - \frac{\Delta x_1}{\sigma})$ at u_1 with

Lagrange remainder, that is,

$$\begin{aligned}
f(u_1 - \frac{\Delta x_1}{\sigma}) &= f(u_1) + f'(u_1)(-\frac{\Delta x_1}{\sigma}) + f''(\xi(\Delta x_1, u_1))\frac{(\Delta x_1)^2}{\sigma^2} \\
&= f(u_1) + u_1 \exp\left(-\frac{1}{2}\|(u_1, \mathbf{u}_{-1})\|^2\right) \frac{\Delta x_1}{\sigma} \\
&\quad + (\xi^2(\Delta x_1, u_1) - 1) \exp\left(-\frac{1}{2}\|(\xi(\Delta x_1, u_1), \mathbf{u}_{-1})\|^2\right) \frac{(\Delta x_1)^2}{\sigma^2}
\end{aligned}$$

where $\xi(\Delta x_1, u_1)$ is between $u_1 - \frac{\Delta x_1}{\sigma}$ and u_1 . On top of that, (a) is derived by

$$\begin{aligned}
&\lim_{\Delta x_1 \rightarrow 0} \int W(\mathbf{x} + \sigma \mathbf{u}) \frac{\exp\left(-\frac{1}{2}\|(u_1 - \frac{\Delta x_1}{\sigma}, \mathbf{u}_{-1})\|^2\right) - \exp\left(-\frac{1}{2}\|(u_1, \mathbf{u}_{-1})\|^2\right)}{\Delta x_1} d\mathbf{u} \\
&= \lim_{\Delta x_1 \rightarrow 0} \int W(\mathbf{x} + \sigma \mathbf{u}) d\mathbf{u} \\
&\quad \cdot \frac{u_1 \exp\left(-\frac{1}{2}\|(u_1, \mathbf{u}_{-1})\|^2\right) \frac{\Delta x_1}{\sigma} + (\xi^2(\Delta x_1, u_1) - 1) \exp\left(-\frac{1}{2}\|(\xi(\Delta x_1, u_1), \mathbf{u}_{-1})\|^2\right) \frac{(\Delta x_1)^2}{\sigma^2}}{\Delta x_1} \\
&= \lim_{\Delta x_1 \rightarrow 0} \int W(\mathbf{x} + \sigma \mathbf{u}) d\mathbf{u} \\
&\quad \cdot \left(\frac{u_1}{\sigma} \exp\left(-\frac{1}{2}\|\mathbf{u}\|^2\right) + (\xi^2(\Delta x_1, u_1) - 1) \exp\left(-\frac{1}{2}\|(\xi(\Delta x_1, u_1), \mathbf{u}_{-1})\|^2\right) \frac{\Delta x_1}{\sigma^2} \right) \\
&\stackrel{(b)}{=} \lim_{\Delta x_1 \rightarrow 0} \int W(\mathbf{x} + \sigma \mathbf{u}) \frac{u_1}{\sigma} \exp\left(-\frac{1}{2}\|\mathbf{u}\|^2\right) d\mathbf{u} \\
&= \int W(\mathbf{x} + \sigma \mathbf{u}) \frac{u_1}{\sigma} \exp\left(-\frac{1}{2}\|\mathbf{u}\|^2\right) d\mathbf{u},
\end{aligned} \tag{8}$$

where (b) is equivalent to the truth of the following equation:

$$\begin{aligned}
&\lim_{\Delta x_1 \rightarrow 0} \left| \Delta x_1 \int W(\mathbf{x} + \sigma \mathbf{u}) (\xi^2(\Delta x_1, u_1) - 1) \exp\left(-\frac{1}{2}\|(\xi(\Delta x_1, u_1), \mathbf{u}_{-1})\|^2\right) d\mathbf{u} \right| \\
&\leq \lim_{\Delta x_1 \rightarrow 0} |\Delta x_1| \cdot |W(\mathbf{x} + \sigma \mathbf{u})| \cdot \left| \int (\xi^2(\Delta x_1, u_1) - 1) \exp\left(-\frac{1}{2}\|(\xi(\Delta x_1, u_1), \mathbf{u}_{-1})\|^2\right) d\mathbf{u} \right| \\
&\leq \lim_{\Delta x_1 \rightarrow 0} |\Delta x_1| \cdot M_W \cdot \left| \int (\xi^2(\Delta x_1, u_1) - 1) \exp\left(-\frac{1}{2}\|(\xi(\Delta x_1, u_1), \mathbf{u}_{-1})\|^2\right) d\mathbf{u} \right| \\
&= \lim_{\Delta x_1 \rightarrow 0} |\Delta x_1| \cdot M_W \cdot \left| \int K(\xi(\Delta x_1, u_1), \mathbf{u}_{-1}) d\mathbf{u} \right| \\
&\leq \lim_{\Delta x_1 \rightarrow 0} |\Delta x_1| \cdot M_W \cdot \int |K(\xi(\Delta x_1, u_1), \mathbf{u}_{-1})| d\mathbf{u}
\end{aligned} \tag{9}$$

where we define $K(s, \mathbf{u}_{-1}) := (s^2 - 1) \exp\left(-\frac{1}{2}\|(s, \mathbf{u}_{-1})\|^2\right)$ with $|s - u_1| \leq \left|\frac{\Delta x_1}{\sigma}\right|$, and we prove (c) by showing that when $|\Delta x_1| < \sigma$, the term

$$\int |K(\xi(\Delta x_1, u_1), \mathbf{u}_{-1})| d\mathbf{u} \leq \int_{s \in [u_1 - \frac{\Delta x_1}{\sigma}, u_1 + \frac{\Delta x_1}{\sigma}]} \max |K(s, \mathbf{u}_{-1})| d\mathbf{u} \tag{10}$$

is bounded: Given the definition of K , there exists a constant $C_K > 1$ such that when $s > C_K$, $|K(s, \mathbf{u}_{-1})|$ is monotone decreasing with respect to s , and when $s < -C_K$, $|K(s, \mathbf{u}_{-1})|$ is monotone increasing with respect to s . Based on that, we discuss the following three cases of the range of u_1 :

1. When $u_1 > 2C_K$, then $s \geq u_1 - \left|\frac{\Delta x_1}{\sigma}\right| > 2C_K - 1 > C_K$, so that $|K(s, \mathbf{u}_{-1})|$ is monotone decreasing with respect to s . Therefore we have

$$\begin{aligned}
&\int_{u_1 > 2C_K} \int_{s \in [u_1 - \frac{\Delta x_1}{\sigma}, u_1 + \frac{\Delta x_1}{\sigma}]} \max |K(s, \mathbf{u}_{-1})| d\mathbf{u} \leq \int_{u_1 > 2C_K} \left| K\left(u_1 - \left|\frac{\Delta x_1}{\sigma}\right|, \mathbf{u}_{-1}\right) \right| d\mathbf{u} \\
&\leq \int_{u_1 > 2C_K} |K(u_1 - 1, \mathbf{u}_{-1})| d\mathbf{u} =: C_1,
\end{aligned}$$

where C_1 is a constant independent of $|\Delta x_1|$.

2. When $-2C_K \leq u_1 \leq 2C_K$, we have

$$\begin{aligned} & \int_{-2C_K \leq u_1 \leq 2C_K} \max_{s \in [u_1 - |\frac{\Delta x_1}{\sigma}|, u_1 + |\frac{\Delta x_1}{\sigma}|]} |K(s, \mathbf{u}_{-1})| du \\ & \leq \int_{-2C_K \leq u_1 \leq 2C_K} \max_{-2C_K \leq u'_1 \leq 2C_K} \left(\max_{s \in [u'_1 - |\frac{\Delta x_1}{\sigma}|, u'_1 + |\frac{\Delta x_1}{\sigma}|]} |K(s, \mathbf{u}_{-1})| \right) du \\ & \leq \int_{-2C_K \leq u_1 \leq 2C_K} \max_{-(2C_K+1) \leq s \leq (2C_K+1)} |K(s, \mathbf{u}_{-1})| du =: C_2 \end{aligned}$$

where C_2 is a constant independent of $|\Delta x_1|$.

3. When $u_1 < -2C_K$, then $s \leq u + |\frac{\Delta x_1}{\sigma}| < -2C_K + 1 < C_K$, so that $|K(s, \mathbf{u}_{-1})|$ is monotone increasing with respect to s . Similar to case 1, we have

$$\begin{aligned} & \int_{u_1 < -2C_K} \max_{s \in [u_1 - |\frac{\Delta x_1}{\sigma}|, u_1 + |\frac{\Delta x_1}{\sigma}|]} |K(s, \mathbf{u}_{-1})| du \leq \int_{u_1 < -2C_K} \left| K(u_1 + \left| \frac{\Delta x_1}{\sigma} \right|, \mathbf{u}_{-1}) \right| du \\ & \leq \int_{u_1 < -2C_K} |K(u_1 + 1, \mathbf{u}_{-1})| du =: C_3 \end{aligned}$$

where C_3 is a constant independent of $|\Delta x_1|$.

Therefore, Equation (10) is bounded by $C_1 + C_2 + C_3$ which is independent of $|\Delta x_1|$, and the proof of Equation (9) is complete. Subsequently, the proof of (b) in Equation (8) is established. Following that, the proof of (a) in Equation (7) is concluded. Consequently, the existence of $\frac{\partial \tilde{W}^\sigma(\mathbf{x})}{\partial x_1}$ is derived from Equation (7).

Continuity of $\frac{\partial \tilde{W}^\sigma(\mathbf{x})}{\partial x_1}$ Given σ , let $Q(\mathbf{x}) := W(\frac{\mathbf{x}}{\sigma})$ and $H(\mathbf{u}) := -u_1 \exp\left(-\frac{1}{2}\|\mathbf{u}\|^2\right)$, according to Equation (7) we have

$$\begin{aligned} \frac{\partial \tilde{W}^\sigma(\mathbf{x})}{\partial x_1} &= \frac{1}{\sigma} \left(\frac{1}{2\pi}\right)^{\frac{n}{2}} \int W(\mathbf{x} + \sigma\mathbf{u}) u_1 \exp\left(-\frac{1}{2}\|\mathbf{u}\|^2\right) d\mathbf{u} \\ &= \frac{1}{\sigma} \left(\frac{1}{2\pi}\right)^{\frac{n}{2}} \int Q(\mathbf{u} + \frac{\mathbf{x}}{\sigma}) H(-\mathbf{u}) d\mathbf{u} \\ &= \frac{1}{\sigma} \left(\frac{1}{2\pi}\right)^{\frac{n}{2}} \int Q(\mathbf{u}) H\left(\frac{\mathbf{x}}{\sigma} - \mathbf{u}\right) d\mathbf{u} \\ &=: \frac{1}{\sigma} \left(\frac{1}{2\pi}\right)^{\frac{n}{2}} C\left(\frac{\mathbf{x}}{\sigma}\right), \end{aligned}$$

where we can see that $C(\frac{\mathbf{x}}{\sigma})$ is a convolution function. As for the continuity of $C(\frac{\mathbf{x}}{\sigma})$, we have:

$$\begin{aligned} \lim_{\mathbf{h} \rightarrow 0} \left| C\left(\frac{\mathbf{x}}{\sigma} + \mathbf{h}\right) - C\left(\frac{\mathbf{x}}{\sigma}\right) \right| &= \lim_{\mathbf{h} \rightarrow 0} \left| \int H\left(\frac{\mathbf{x}}{\sigma} + \mathbf{h} - \mathbf{u}\right) Q(\mathbf{u}) d\mathbf{u} - \int H\left(\frac{\mathbf{x}}{\sigma} - \mathbf{u}\right) Q(\mathbf{u}) d\mathbf{u} \right| \\ &\leq \lim_{\mathbf{h} \rightarrow 0} \int \left| H\left(\frac{\mathbf{x}}{\sigma} + \mathbf{h} - \mathbf{u}\right) - H\left(\frac{\mathbf{x}}{\sigma} - \mathbf{u}\right) \right| |Q(\mathbf{u})| d\mathbf{u} \\ &\stackrel{(a)}{\leq} \lim_{\mathbf{h} \rightarrow 0} M_W \int \left| H\left(\frac{\mathbf{x}}{\sigma} + \mathbf{h} - \mathbf{u}\right) - H\left(\frac{\mathbf{x}}{\sigma} - \mathbf{u}\right) \right| d\mathbf{u} \\ &\stackrel{(b)}{=} 0, \end{aligned}$$

where (a) holds because $Q_\sigma(\mathbf{x}) := W(\frac{\mathbf{x}}{\sigma})$ is bounded by $M_W := \max_{\mathbf{x}} W(\mathbf{x})$, and (b) holds because $H(\mathbf{u})$ is integrable. As a result, $C(\frac{\mathbf{x}}{\sigma})$ is continuous with respect to \mathbf{x} , and then $\frac{\partial \tilde{W}^\sigma(\mathbf{x})}{\partial x_1}$ is also continuous with respect to x_1 .

Differentiability of \tilde{W}^σ From the preceding discussion, it is evident that $\tilde{W}^\sigma(\mathbf{x})$ is differentiable with respect to x_1 . This technique can be extended straightforwardly to x_2, x_3, \dots, x_n . Therefore, $\tilde{W}^\sigma(\mathbf{x})$ is differentiable (and thus continuous) with respect to \mathbf{x} . \square

Proof of Proposition 4.1. $\tilde{Z}_S^\sigma(e^\alpha, \lambda)$ is defined as the Gaussian smoothing approximation of $Z_S(e^\alpha, \lambda)$, whose range is $[\min_{V \in \mathcal{S}} \min_{A \in \mathcal{A}} \sum_{i=1}^n v_i(A), \max_{V \in \mathcal{S}} \max_{A \in \mathcal{A}} \sum_{i=1}^n v_i(A)]$. Therefore, the proof is done by applying Lemma B.1. \square

C Further Implementation Details

We use the same hyperparameters for OD-VVCA and the ablation version FO-VVCA in all the settings, and we list the main hyperparameters in Table 2.

Table 2: Hyperparameters of OD-VVCA and FO-VVCA.

(a) Small-scale settings.

Hyperparameter	Symmetric					Asymmetric				
	2×2(A)	2×5(A)	3×10(A)	2×2(D)	3×10(D)	5×3(B)	3×10(B)	2×5(C)	5×3(C)	3×10(C)
Learning Rate	0.01	0.001	0.001	0.01	0.001	0.001	0.001	0.001	0.001	0.001
n_r	8	8	8	8	8	8	8	8	8	8
σ	0.01	0.01	0.01	0.01	0.01	0.01	0.01	0.01	0.01	0.01
Iteration	2000	2000	2000	2000	2000	2000	2000	2000	2000	2000
Batch Size	1024	2048	1024	1024	1024	1024	1024	2048	1024	1024

(b) Large-scale settings.

Hyperparameter	Symmetric				Asymmetric					
	5×10(A)	10×5(A)	5×10(D)	10×5(D)	5×10(B)	10×5(B)	30×5(B)	5×10(C)	10×5(C)	30×5(C)
Learning Rate	0.0003	0.0003	0.0003	0.0003	0.005	0.005	0.005	0.005	0.005	0.005
n_r	8	8	8	8	8	8	8	8	8	8
σ	0.001	0.01	0.01	0.01	0.01	0.01	0.01	0.01	0.01	0.01
Iteration	2000	2000	2000	2000	2000	2000	2000	2000	2000	2000
Batch Size	1024	1024	1024	1024	1024	1024	1024	1024	1024	1024

For Lottery AMA [Curry et al., 2023] and AMenuNet [Duan et al., 2023], we adopt the same hyperparameters as those specified in their original publications, with the exception of the candidate size. Due to computational resource limitations, the size of the candidate allocation set cannot be excessively large. Therefore, we set the candidate size based on the complexity of the auction scenario to make a balance between performance and computational feasibility, as detailed in Table 3.

Table 3: Candidate size of Lottery AMA and AMenuNet in different settings.

(a) Small-scale settings.

Method	Symmetric					Asymmetric				
	2×2(A)	2×5(A)	3×10(A)	2×2(D)	3×10(D)	5×3(B)	3×10(B)	2×5(C)	5×3(C)	3×10(C)
Lottery AMA	32	128	1024	32	1024	128	1024	128	128	1024
AMenuNet	32	128	1024	32	1024	128	1024	128	128	1024

(b) Large-scale settings.

Method	Symmetric				Asymmetric					
	5×10(A)	10×5(A)	5×10(D)	10×5(D)	5×10(B)	10×5(B)	30×5(B)	5×10(C)	10×5(C)	30×5(C)
Lottery AMA	4096	4096	4096	4096	4096	4096	4096	4096	4096	4096
AMenuNet	4096	4096	4096	4096	4096	4096	4096	4096	4096	4096

D Training Time

We document the total training time of Lottery AMA [Curry et al., 2023], AMenuNet [Duan et al., 2023], BBBVCA [Sandholm and Likhodedov, 2015], and the proposed OD-VVCA for different auction scales in Table 4. We tuned the number of training iterations for each method based on our empirical observations of their convergence rates, which are also listed in the table.

Table 4: The total training time for different methods. We use the same parallelizable dynamic programming for winning allocation determination in both BBBVCA and OD-VVCA.

Training Time	2×2	2×5	5×3	10×5	30×5	3×10	5×10
Lottery AMA (10000 iterations)	1min40s	15min	8min	20min	6h	1h40min	9h
AMenuNet (1000 iterations)	12min	22min	24min	1h20min	50min*	1h20min	3h30min
BBBVCA (4000 iterations)	1min	3min	3min	16min	1h	2h	4h20min
OD-VVCA (2000 iterations)	1min20s	7min	6min	40min	3h	6h	9h

*We reduce the batch size of AMenuNet in the 30×5 scenarios due to GPU constraints.

As indicated in the table, OD-VVCA demonstrates acceptable training times across all settings. This result, along with the similarly acceptable training times of BBBVCA, underscores the efficiency of the parallelized dynamic programming winner determination algorithm. Furthermore, the relatively small number of iterations highlights the effective convergence of our objective decomposition method.